Collision Potential Analysis in First and Second Order Integrator Networks Over Strongly Connected Digraphs

Chengda Ji and Dennice F. Gayme

Abstract—This paper investigates the collision potential of any two nodes in first and second order integrator networks subject to distributed disturbances. Our results extend previous analysis quantifying this notion of robustness using an induced L_2 to L_∞ norm for networks with symmetric feedback interconnection to systems with directed feedback. We focus on the special case where the underlying feedback interconnection is represented by a strongly connected digraph described by a diagonalizable weighted graph Laplacian matrix. We derive analytical expressions for system robustness for networks of first and second order systems with two different combinations of absolute and relative state feedback. A numerical example simulating a second order system connected over a line graph (a vehicle platoon) is employed to investigate the effect of asymmetric feedback control laws on collision potential. Our numerical results show that in contrast to previous results showing improved stability margin through asymmetric feedback control laws, this type of control law can actually increase the collision potential (decrease system robustness) for certain vehicle pairs in platoons with and without leaders.

I. INTRODUCTION

A large number of networks can be modeled as first or second order integrator systems connected over one or more directed graphs. These systems are typically evaluated in terms of their stability. For first order systems, stability is commonly defined in terms of the ability to reach consensus, e.g., to achieve some coordinated behavior in a first order robotic network [1]. The stability of second order systems is often defined in terms of the application of interest, e.g., synchronization in power systems [2], [3], [4] or biological networks [5], or string stability in vehicle platoons [6], [7]. Another measure of interest is the error decay rate, which can be quantified through the real part of the least stable eigenvalue (stability margin) [8], [9].

Performance of networked systems can likewise be evaluated using a number of metrics including the long range disorder (e.g. steady-state variance of each state) [10], [11], [12], or the L_2 to L_2 gain from a disturbance input to the system states (which the authors referred to as the L_2 gain) [13]. System performance has also been extensively studied in terms of various notions of system robustness. For example, [13] focused on how communication errors affected leader-follower consensus using the L_2 gain described above. [14] explored the impact of additive and measurement noise on the input-output \mathcal{H}_2 norm of the system, whereas [15] investigated robustness of linear systems with respect to δ -correlated stochastic disturbances.

Chengda Ji and D. F. Gayme are with Dept. of Mechanical Engineering, Johns Hopkins University, 3400 N. Charles St., Baltimore, MD 21218 USA chengdaji@jhu.edu, dennice@jhu.edu

Recent work [16] introduced the notion of collision potential between two network nodes as a measure of robustness in vehicle networks under a variety of feedback control laws. In that work, collision potential was quantified in terms of an L_2 to L_{∞} induced norm, which was shown to be equivalent to an \mathcal{H}_2 norm for the special case of a single output bounded input bounded output system. They used this framework to derive the maximum permissible disturbance energy that ensures that no two vehicles in the network collide for the special case of symmetric feedback interconnection structures. Asymmetry has been shown to increase the stability margin for the special case of vehicle networks connected over line graphs (vehicle platoons) [9]. Therefore it is of interest to extend the results in [16] to systems with asymmetric feedback to investigate if similar performance gains can be achieved.

This paper takes a step toward to general asymmetric networks by extending the analysis framework in [16] to a special class of asymmetric control laws; those whose underlying graph structure is described by a diagonalizable weighted graph Laplacian matrix. These results extend a subset of the results in [17], which considered systems whose interconnection structures emit normal graph Laplacians. We first extend the \mathcal{H}_2 norm computations in [16] to evaluate the collision potential of a critical node pair in single and double integrator networks for systems connected over digraphs described by diagonalizable weighted graph Laplacians. For the second order systems, we obtain closed form solutions for systems with two different feedback laws; (1) relative position and absolute velocity (RPAV) control and (2) relative position and relative velocity (RPRV) control.

We illustrate the theory through a simulation study of second order systems connected over a line graph as a model of vehicle platoons. We then investigate collision potential between vehicle pairs for networks with RPAV and RPRV control laws in platoons with and without leaders. Our results show that while asymmetric feedback control laws improve the stability margin, as found in [9], they also increase the potential that certain vehicle pairs will collide in platoons with and without leaders. Therefore there is a trade-off between stability and this type of robustness in these systems.

The remainder of this work is organized as the follows. Section II describes the mathematical background and notation used throughout the work. Section III provides the models for the first and second order integrator networks along with their corresponding feedback laws. That section also describes the single system output that enables the computation of collision potential through the L_2 to L_{∞}

induced \mathcal{H}_2 norm. Section IV presents the main theoretical results; closed form solutions for the \mathcal{H}_2 norm based measure of collision potential for a first order system, and for second order systems with RPAV and RPRV control laws. A numerical investigation for the special case of second order systems connected over a line graph (i.e., a linear vehicle platoon) is provided in Section V. We conclude the paper in Section VI.

II. PRELIMINARIES

For a complex number x = a + bi, Re(x) = a and Im(x) = b respectively denote the real and complex parts of $x. \ \bar{x} = a - bi$ represents the conjugate of $x. \ \mathbf{0}_{n \times n} \in \mathbb{R}^{n \times n}$ and $I_{n\times n}\in\mathbb{R}^{n\times n}$ respectively denote an $n\times n$ matrix with all elements equal to zero, and an $n \times n$ identity matrix. Given $A \in \mathbb{C}^{n \times n}$, we denote its inverse as A^{-1} , i.e., $AA^{-1} = I_{n \times n}$. The conjugate transpose of matrix A is denoted as A^* . For a real matrix A, we denote the transpose of A by A^T , and the inverse of the transpose as $A^{-T} = (A^{T})^{-1} = (A^{-1})^{T}$. Given a matrix T, $[T]_{pq}$ denotes the element in its p^{th} row and q^{th} column. tr(T)denotes the trace of matrix T. $\mathbf{1}_n \in \mathbb{R}^n$ is a column vector with all elements equal to 1. $\mathbf{0}_n \in \mathbb{R}^n$ is a column vector with with all elements equal to 0. Given a set of numbers $S = \{s_1 \ s_2 \ \cdots \ s_n\}, \ diag(S) \in \mathbb{C}^{n \times n} \ \text{is a diagonal matrix}$ with the ordered elements of S along its main diagonal.

We define an undirected graph as an ordered pair, denoted $\mathcal{G}=(N,\mathcal{E})$, where N is the set of nodes and \mathcal{E} is the set of unordered pairs of nodes $\{i,j\}$ called edges. A weighted directed graph (digraph) is denoted as $\mathcal{G}=(N,\mathcal{E},W)$, where the N is the set of nodes, \mathcal{E} is the set of ordered pairs of nodes (i,j) describing directed edges and W is a set of nonnegative weights $w_{(i,j)}$, for ordered node pairs (i,j). If there is no directed edge connecting node i to node j, i.e., $(i,j) \notin \mathcal{E}$, $w_{(i,j)}=0$, otherwise, the weight is a strictly positive number, i.e., $w_{(i,j)}>0$. A path is an ordered sequence of graph nodes such that any pair of consecutive nodes in the sequence is an edge of the graph. If there is a directed path from any node to any other node in a directed graph \mathcal{G} , then we say this graph is strongly connected.

Given a weighted digraph $\mathcal{G} = (N, \mathcal{E}, W)$, the associated weighted Laplacian matrix is

$$[L]_{ij} = \begin{cases} -w_{(i,j)}, & \text{if } i \neq j; \\ \sum_{h=1, h \neq i}^{n} w_{(i,h)}, & \text{otherwise,} \end{cases}$$

where $w_{(i,j)}$ is the weight attributed to the edge between nodes i and j. λ_i denotes the i^{th} eigenvalue of L where $0 = \lambda_1 \leq Re(\lambda_2) \leq \cdots \leq Re(\lambda_n)$. Finally, we define the $n \times n$ matrix $T = \begin{bmatrix} t_1 & t_2 & \cdots & t_n \end{bmatrix}$ whose i^{th} column t_i is the eigenvector associated with $\lambda_i(L)$, therefore $t_1 = \frac{1}{n} \mathbf{1}_n$.

III. PROBLEM SETUP

In this section, we introduce the first and second order systems of interest along with their respective feedback control laws. As in [16], we utilize two different types interconnection graphs for each type of system. The first type of interconnection graph describes the feedback structure. We

refer to this graph as the communication graph and denote it as $\mathcal{G}=(N,\mathcal{E},W)$, where \mathcal{E} are directed edges defined as the node pairs $(u,v)\in\mathcal{E}$, where information flows from node u to node v. The second type of graph describes the physical system interconnection, and we refer to it as the collision graph, denoted $\mathcal{G}_c=(N,\mathcal{E}_c)$. The collision graph has undirected edges $\mathcal{E}_c\in\mathcal{G}_c$ given by the node pairs $\{j,k\}\in\mathcal{E}_c$ for which the vehicles at nodes j and k may collide. See [16] for a discussion regarding construction of the collision graph.

To characterize collisions we further define a nominal spacing between vehicles (or robots) i and j, denoted by h_{ij} , in a manner similar to [16]. If we consider a network connected over a line graph with vehicle (robot) i immediately in front of vehicle (robot) j, then this h_{ij} is the distance between the front of vehicle (robot) j and the back of vehicle (robot) i. More generally, we denote the closed and connected region that a vehicle (robot) resides in as V_i , which leads to

$$h_{ij} = \min |x_i^* - x_j^*|$$

for points $x_i^* \in V_i$ and $x_j^* \in V_j$. If j is in front of i, then $h_{ij} - x_i + x_j \leq 0$ means that vehicles (robots) i and j have collided

We consider input-output linear systems G of the form

$$\dot{\phi} = A\phi + Bw \tag{1a}$$

$$y = C\phi$$
, (1b)

where $x \in \mathbb{R}^n$, $A \in \mathbb{R}^{n \times n}$, $w \in \mathbb{R}^m$, $B \in \mathbb{R}^{n \times m}$, $y \in \mathbb{R}^p$ and $C \in \mathbb{R}^{p \times m}$. We next specify the state, input and output matrices for the systems of interest.

1) First Order Systems: We consider single integrator systems with the dynamics at node $i \in N$ given by

$$\dot{x}_i = u_i + w_i, \tag{2}$$

where

$$u_i = -\sum_{(i,j)\in\mathcal{E}} \alpha_{ij} (x_i - x_j)$$

is the control input for node i, and w_i is the disturbance at that node. This type of model can be used to represent a robotic network [1]. As in [16], we define the output in terms of the relative state value for the two critical nodes of interest $\{i,j\} \in \mathcal{E}_c$ such that $y=x_i-x_j$. We can then represent the first order input-output system as

$$\dot{x} = -Lx + I_{n \times n} w \tag{3a}$$

$$y = Cx, (3b)$$

where $x \in \mathbb{R}^n$, and the state matrix $A = -L \in \mathbb{R}^{n \times n}$ is a weighed graph Laplacian matrix determined by the underlying communication graph \mathcal{G} . The output matrix is given by

$$C = \begin{bmatrix} 0 & \cdots & 1 & 0 & \cdots & -1 & 0 & \cdots \end{bmatrix}, \qquad (4)$$

where 1 and -1 are in i^{th} and j^{th} position of matrix C respectively.

2) Second Order Systems: Second order systems are widely used to describe vehicle networks. The dynamics at each node $i \in N$ in such systems is given by

$$\ddot{x}_i = u_i + w_i, \tag{5}$$

where the form of u_i is determined the feedback interconnection structure. Second order systems can have two communication graphs respectively associated with their position and velocity feedback interconnection structure, we denote these by $\mathcal{G}_x = (N_x, \mathcal{E}_x, W_x)$ and $\mathcal{G}_v = (N_v, \mathcal{E}_v, W_v)$, respectively. In the present work we focus on the two feedback control laws proposed in [10], 1) relative position and absolute velocity (RPAV) control and 2) relative position and relative velocity (RPRV) control.

For the RPAV control strategy, the control input at node i is given by

$$u_i = -\sum_{(i,j)\in\mathcal{E}_x} \alpha_{ij} (x_i - x_j) - \dot{x}_i, \tag{6}$$

where the feedback law is based on the relative position of nodes i and j for each edge $(i,j) \in \mathcal{E}_x$ and a local velocity measurement relative to a global reference. We refer to this type of velocity measure as absolute velocity feedback. The corresponding state space representation is

$$\begin{bmatrix} \dot{x} \\ \dot{v} \end{bmatrix} = \begin{bmatrix} \mathbf{0}_{n \times n} & I_{n \times n} \\ -L_{\alpha} & -I_{n \times n} \end{bmatrix} \begin{bmatrix} x \\ v \end{bmatrix} + \begin{bmatrix} \mathbf{0}_{n \times n} \\ I_{n \times n} \end{bmatrix} w$$
 (7a)

$$y = \begin{bmatrix} H & \mathbf{0}_n^T \end{bmatrix} \begin{bmatrix} x \\ v \end{bmatrix}, \tag{7b}$$

where H is of the form (4), i.e. the output measures the relative distance between nodes i and j.

For systems under RPRV control the input at node i is given by

$$u_i = -\sum_{(i,j)\in\mathcal{E}_x} \alpha_{ij} (x_i - x_j) - \sum_{(i,j)\in\mathcal{E}_v} \beta_{ij} (\dot{x}_i - \dot{x}_j). \quad (8)$$

The corresponding state space form is

$$\begin{bmatrix} \dot{x} \\ \dot{v} \end{bmatrix} = \begin{bmatrix} \mathbf{0}_{n \times n} & I_{n \times n} \\ -L_{\alpha} & -L_{\beta} \end{bmatrix} \begin{bmatrix} x \\ v \end{bmatrix} + \begin{bmatrix} 0_{n \times n} \\ I_{n \times n} \end{bmatrix} u \tag{9a}$$

$$y = \begin{bmatrix} H & \mathbf{0}_n^T \end{bmatrix} \begin{bmatrix} x \\ v \end{bmatrix}, \tag{9b}$$

where L_{α} and L_{β} are Laplacian matrices corresponding to the respective position and velocity communication graphs, \mathcal{G}_x and \mathcal{G}_v respectively.

IV. ANALYTICAL RESULTS

We now demonstrate how to extend the analysis in [16] to directed graphs. Theorem 1 in [16] proved that if

$$||w||_{\mathcal{L}_2} < \min_{i,j \in \mathcal{E}_c} \frac{h_{ij}}{\sqrt{P_{ij}}},\tag{10}$$

for nominal spacing h_{ij} , then will be no collisions in the network. Here P_{ij} is the nodal performance between node pair i and j that was derived in [12] for symmetric communication graphs. They further showed that this nodal performance P_{ij}

can be computed as the \mathcal{H}_2 norm for the single output defined for the systems (3), (7) and (9). Therefore given nominal vehicle (or robot) spacings h_{ij} the collision potential of the platoon can be evaluated by computing the \mathcal{H}_2 norm of the system. Based on (10) a higher \mathcal{H}_2 norm indicates lower disturbance capacity.

The \mathcal{H}_2 norm, and equivalently P_{ij} in (10), can be interpreted as the sum of the time integrals of the output response powers due to an impulse disturbance input at each node [3]

$$||G||_{H_2}^2 = tr\left(B^T \int_0^\infty e^{A^T t} C^T C e^{At} dt B\right).$$
 (11)

The next subsections provide closed form expressions for the \mathcal{H}_2 norms (that provide measures of collision potential) for the first order system (3) as well as the second order systems with RPAV and RPRV control laws, respectively described in equations (7) and (9).

A. First order systems

For a strongly connected graph, the corresponding Laplacian matrix has only one zero eigenvalue. This condition enables us to state the following theorem.

Theorem 4.1: Given a first order system (3) with communication graph $\mathcal{G} = (N, \mathcal{E}, W)$ and collision graph $\mathcal{G}_c = (N_c, \mathcal{E}_c)$. If \mathcal{G} is strongly connected and the corresponding Laplacian matrix L is diagonalizable, the \mathcal{H}_2 norm of this first order system is given by

$$||G||_{H_2}^2 = tr\left((T^{-1})^*\hat{X}T^{-1}\right),\tag{12a}$$

$$\left[\hat{X}\right]_{ls} = \begin{cases} 0, & l \text{ or } s = 1, \\ -(\bar{t_{il}} - \bar{t_{jl}})(t_{is} - t_{js}), & otherwise, \end{cases}$$
(12b)

where $\{i,j\} \in \mathcal{E}_c$. T is a invertible matrix that diagonalizes the Laplacian matrix, i.e., $-L = T\Lambda T^{-1}$, $t_{pq} = [T]_{pq}$, $[\Lambda]_{ii} = \lambda_i$, and the eigenvalues are sorted as $Re(\lambda_1) \geq Re(\lambda_2) \geq \cdots \geq Re(\lambda_n)$.

Proof: With \mathcal{G} strongly connected, $0=\lambda_1>Re(\lambda_2)\geq\cdots\geq Re(\lambda_n)$. The first column of matrix T is $t_1=\frac{1}{n}\mathbf{1}_n\in\mathbb{R}^n$ which is associated with the zero eigenvalue. As there is a zero in its spectrum, the \mathcal{H}_2 norm of this system may not exist. We therefore first prove the existence of this norm for our problem. Representing (11) in terms of the decomposition of L leads to

$$\begin{split} \left\|G\right\|_{H_2}^2 &= tr\left(\int_0^\infty (Ce^{At}B)^TCe^{At}Bdt\right) \\ &= tr\left((T^{-1})^*\int_0^\infty e^{\Lambda t}T^*C^TCTe^{\Lambda t}dtT^{-1}\right). \end{split}$$

As $Ct_1 = \mathbf{0}_n$, we have

$$T^*C^TCT = \begin{bmatrix} 0 & \mathbf{0}_{n-1}^T \\ \mathbf{0}_{n-1} & (T^*C^TCT)_* \end{bmatrix},$$

in which $(T^*C^TCT)_* \in \mathbb{R}^{n \times n}$ is a principle submatrix of T^TC^TCT . Direct computation of $e^{\Lambda t}T^TC^TCTe^{\Lambda t}$ shows that the elements associated with the zero eigenvalue (first

row and first column of T^*C^TCT) are all 0. Thus the zero eigenvalue will not contribute to the \mathcal{H}_2 norm, and the integral in (11) exists.

Next we prove that the form in (12) is correct. Notice that

$$[(CT)^*(CT)]_{ls} = (\bar{t_{il}} - \bar{t_{jl}})(t_{is} - t_{js}),$$

we have

$$\begin{split} \left[e^{\Lambda^*t}T^TC^TCTe^{\Lambda t}\right]_{ls} &= \\ \begin{cases} 0, & l \ or \ s=1, \\ (\bar{t_{il}} - \bar{t_{jl}})(t_{is} - t_{js})e^{\bar{\lambda_l} + \lambda_s}, & otherwise \end{cases} \end{split}$$

Thus we can find $\forall l, s \neq 1$.

$$\begin{split} \left[\hat{X}\right]_{ls} &= \int_0^\infty (\bar{t_{il}} - \bar{t_{jl}})(t_{is} - t_{js})e^{\bar{\lambda}_l t + \lambda_s t} dt \\ &= \frac{-(\bar{t_{il}} - \bar{t_{jl}})(t_{is} - t_{js})}{\bar{\lambda}_l + \lambda_s}. \end{split}$$

B. Second order systems

For second order systems we present the results in terms of the two control strategies.

The first theorem provides a result analogous to that in Theorem 4.1 for second order systems under RPAV control.

Theorem 4.2: Given a second order system under the **RPAV** control strategy as described in (7). If the communication graph \mathcal{G}_x is strongly connected and the corresponding Laplacian $-L_{lpha}$ is diagonalizable, the \mathcal{H}_2 norm of the corresponding system is given by

$$\|G_{\alpha}\|_{H_{2}}^{2}=tr\left((P^{-1}T_{diag}^{-1}B)^{*}\hat{X}(P^{-1}T_{diag}^{-1}B)\right), \quad \text{(13a)}$$

where

$$P = EFR$$
.

$$\left[\hat{X} \right]_{ls} = \begin{cases} 0, & l \text{ or } s \leq 2, \\ \frac{-1}{\bar{\delta}_l + \delta} \bar{q}_l q_s, & otherwise. \end{cases}$$
 (13b)

$$q_l = [CT_{diag}P]_l, (13c)$$

Specifically, T_{diag} is a block diagonal matrix

$$T_{diag} = \begin{bmatrix} T & \\ & T \end{bmatrix}, \tag{14}$$

where T is the matrix that diagonalizes $-L_{\alpha} = T\Lambda T^{-1}$. $[\Lambda]_{ii} = \lambda_i$, and the sequence λ_i is sorted as $0 = \lambda_1 > 1$ $Re(\lambda_2) \geq \cdots \geq Re(\lambda_n)$. E is a permutation matrix such

$$E = [e_1 \ e_{n+1} \ e_2 \ e_{n+2} \ \cdots \ e_i \ e_{i+n} \ \cdots \ e_n \ e_{2n}], (15)$$

where $e_i \in \mathbb{R}^{2n}$ is a standard basis vector, i.e., it has a one as the i^{th} element and all other elements are zeros. Matrix F is a block diagonal matrix

$$F = \begin{bmatrix} F_1 & & \\ & \ddots & \\ & & F_n \end{bmatrix}, \tag{16}$$

where $F_1 = I_{2\times 2}$ and $F_i = \begin{bmatrix} 1 & 0 \\ 0 & \sqrt{\lambda_i} \end{bmatrix}$, $\forall i \neq 1$. R is another a block diagonal matrix such that

$$R = \begin{bmatrix} R_1 & & \\ & \ddots & \\ & & R_n \end{bmatrix}, \tag{17}$$

$$\begin{bmatrix} T^TC^TCTe^{\Lambda t} \end{bmatrix}_{ls} = \qquad \qquad \text{where} \qquad R_1 = \begin{bmatrix} 1 & -\frac{\sqrt{2}}{2} \\ 0 & \frac{\sqrt{2}}{2} \end{bmatrix} \text{ and } \qquad R_i = \begin{bmatrix} 0, & & & & & \\ (t_{il} - t_{jl})(t_{is} - t_{js})e^{\bar{\lambda}_l + \lambda_s}, & \text{otherwise.} \end{bmatrix} \begin{bmatrix} -\frac{-1 + \sqrt{1 + 4\lambda_i}}{2\sqrt{\lambda_i}} & -\frac{-1 - \sqrt{1 + 4\lambda_i}}{2\sqrt{\lambda_i}} \\ 1 & & & & 1 \end{bmatrix}, \ \forall i \neq 1. \ \text{With}$$

only $\lambda_1 = 0$, it is easy to verify that matrix R is invertible. The values $\delta_i = [\Delta]_{ii}$ are the diagonal elements of the block diagonal matrix

$$\Delta = \begin{bmatrix} \Delta_1 & & \\ & \ddots & \\ & & \Delta_n \end{bmatrix}, \tag{18}$$

with
$$\Delta_1 = \begin{bmatrix} 0 & 0 \\ 0 & 1 \end{bmatrix}$$
 and $\Delta_i = \begin{bmatrix} \frac{-1 - \sqrt{1 + 4\lambda_i}}{2} \\ \frac{-1 + \sqrt{1 + 4\lambda_i}}{2} \end{bmatrix}$, $\forall i \neq 1$.

Proof: First we diagonalize the state matrix

$$A = T_{diag} EFR \Delta R^{-1} F^{-1} E^T T_{diag}^{-1}.$$

Since the first element of Δ (which is an the eigenvalue of A) is zero, the \mathcal{H}_2 norm may not exist. Therefore analogous to the proof of Theorem 4.1, we need to verify the existence of the \mathcal{H}_2 norm. From (11), we have

$$\|G_{\alpha}\|_{H_{2}}^{2} = tr(\hat{P}^{*} \int_{0}^{\infty} e^{\Delta^{*}t} P^{*} T_{diag}^{*} C^{*} C T_{diag} P e^{\Delta t} dt \ \hat{P}), \tag{19}$$

$$\hat{P} = P^{-1} T_{diag}^{-1} B.$$

In particular

$$CT_{diag}E = [t_{i1}-t_{j1} \ 0 \ t_{i2}-t_{j2} \ \cdots \ 0 \ t_{in}-t_{jn}].$$

As the first column of T is $t_1 = \frac{1}{n} \mathbf{1}_n$, thus

$$CT_{diag}E = \begin{bmatrix} 0 & 0 & t_{i2} - t_{j2} & \cdots & 0 & t_{in} - t_{jn} \end{bmatrix}.$$

With F and R as block diagonal matrices, we have

$$CT_{diag}P = CT_{diag}EFR = q = \begin{bmatrix} 0 & 0 & h_{2n-2} \end{bmatrix}.$$
 (20)

Therefore the integration associated with eigenvalue $\delta_1=0$ is zero and the \mathcal{H}_2 norm exists. We then recover the form of (13) by substituting (20) into (19).

Compared with RPAV control, the existence of relative velocity feedback in the RPRV control law introduces a second communication graph \mathcal{G}_v . The following theorem describes the form of the \mathcal{H}_2 norm for RPRV control.

Theorem 4.3: Given a second order system under the **RPRV** control strategy as described in (8). If the communication graphs of position and velocity, respectively \mathcal{G}_x and \mathcal{G}_v , are strongly connected and their corresponding Laplacian matrices $-L_{\alpha}$ and $-L_{\beta}$ are simultaneously diagonalizable, the \mathcal{H}_2 norm of this second order system can be represented as

$$\|G_{\alpha\beta}\|_{H_2}^2 = tr\left((P^{-1}T_{diag}^{-1}B)^*\hat{X}(P^{-1}T_{diag}^{-1}B)\right),$$
 (21a)

P = EFR;

$$\left[\hat{X} \right]_{ls} = \begin{cases} 0, & l \text{ or } s \leq 2, \\ \frac{-1}{\bar{\delta_l} + \delta_s} \bar{q_l} q_s, & otherwise; \end{cases}$$
 (21b)

$$q_l = [CT_{diag}P]_l. (21c)$$

In particular, T_{diag} is of the form (14), with matrix T that can diagonalize both $-L_{\alpha}$ and $-L_{\beta}$, e.g., $-L_{\alpha} = T\Lambda_{\alpha}T^{-1}$ and $-L_{\beta} = T\Lambda_{\beta}T^{-1}$, with $[\Lambda_{\alpha}]_{ii} = \lambda_{i}^{\alpha}$ and $[\Lambda_{\beta}]_{ii} = \lambda_{i}^{\beta}$. λ_{i}^{α} is sorted as $0 = \lambda_{1}^{\alpha} > Re(\lambda_{2}^{\alpha}) \geq \cdots \geq Re(\lambda_{n}^{\alpha})$. E is given by (15). The matrix F is obtained by substituting $\lambda_{i} = \lambda_{i}^{\alpha}$ into (16). Matrix R is a block diagonal matrix defined in (17), with $R_{1} = I_{n \times n}$ and

$$R_{i} = \begin{bmatrix} -\frac{\lambda_{i}^{\beta} + \sqrt{(\lambda_{i}^{\beta})^{2} + 4\lambda_{i}^{\alpha}}}{2\sqrt{\lambda_{i}^{\alpha}}} & -\frac{\lambda_{i}^{\beta} - \sqrt{(\lambda_{i}^{\beta})^{2} + 4\lambda_{i}^{\alpha}}}{2\sqrt{\lambda_{i}^{\alpha}}} \\ 1 & 1 \end{bmatrix}, \ \forall i \neq 1.$$

 δ_k is the k^{th} diagonal element of a block diagonal matrix Δ which is of the form of (18) but with different entries. In particular, for this case $\Delta_1 = \begin{bmatrix} 0 & 1 \\ 0 & 0 \end{bmatrix}$ is a 2×2 Jordan block associated with 0s and

$$\Delta_{i} = \begin{bmatrix} \frac{\lambda_{i}^{\beta} - \sqrt{(\lambda_{i}^{\beta})^{2} + 4\lambda_{i}^{\alpha}}}{2} \\ \frac{\lambda_{i}^{\beta} + \sqrt{(\lambda_{i}^{\beta})^{2} + 4\lambda_{i}^{\alpha}}}{2} \end{bmatrix}, \forall i \neq 1.$$

Proof: A Laplacian matrix whose zero eigenvalue has algebraic and geometric multiplicity one, always has the corresponding eigenvector $\frac{1}{n}\mathbf{1}_n$. Since L_α and L_β are strongly connected and simultaneously diagonalizable by T, if $\lambda_1^\alpha=0$, then $t_1=\frac{1}{n}\mathbf{1}_n$, and $\lambda_1^\beta=0$. Based on this statement, we can locate the position of the zero eigenvalue in Λ_β and block diagonalize

$$A = T_{diag}EFR\Delta R^{-1}F^{-1}E^{T}T_{diag}^{-1}.$$

such that Δ is the block diagonal matrix with all of the eigenvalues of A on its main diagonal and Δ_1 is a Jordan block associated with the two 0 eigenvalues. In order to compute the \mathcal{H}_2 using (19) we first need to prove that the \mathcal{H}_2 norm exists. By explicitly computing $CT_{diag}Pe^{\Delta t}$ using (20), one can show that the elements in $CT_{diag}P$ associated with the zero eigenvalues in Δ are 0. Therefore these 0 eigenvalues do not contribute to the \mathcal{H}_2 norm and the norm exists. The desired result (21) can then be obtained using (19).

C. Application to line graphs

In this section we discuss the special case of networks whose communication interconnection structure is represented by a line graph. In particular, we show that the weighted Laplacians associated with the corresponding directed graphs are diagonalizable. Figure 1 provides an example of such system consisting of a vehicular network with 4 nodes in both the communication and collision graphs. The solid line represents the communication graph for position and velocity feedback, $\mathcal{G}_x = \mathcal{G}_v = (N, \mathcal{E}, W)$ with edge set $\mathcal{E} = \{(1,2), (2,1), (2,3), (3,2), (3,4), (4,3)\}$. The dashed line represents the collision graph, $\mathcal{G}_c = (N_c, \mathcal{E}_c)$, which has the edge set $\mathcal{E}_c = \{\{1,2\}, \{2,3\}, \{3,4\}\}$.



Fig. 1: A vehicular network example with line graph structure

We now introduce the graph Laplacians for the symmetric and asymmetric gain structures for these linear networks. Given a weighted line graph with n nodes, the corresponding Laplacian matrix with symmetric gains is given by

$$L_{sym} = \begin{bmatrix} 1 & -1 \\ -1 & 2 & -1 \\ & \ddots & \ddots & \ddots \\ & & -1 & 2 & -1 \\ & & & -1 & 1 \end{bmatrix} . \tag{22}$$

For the assymetric systems we focus on a special class of asymmetry in which the sum of asymmetric gains for a given edge pair (along a particular edge in the graph) have equal offsets (ϵ positive in one direction and negative in the other). Therefore the sum of the bidirectional communication remains the same for either a symmetric or an asymmetric graph with nominal edge weights 1. For example if the control gain from node i to node j is $1+\epsilon$ then the gain from node j to node j t

$$L_{asym} = \begin{bmatrix} 1 - \epsilon & -1 + \epsilon \\ -1 - \epsilon & 2 & -1 + \epsilon \\ & \ddots & \ddots & \ddots \\ & & -1 - \epsilon & 2 & -1 + \epsilon \\ & & & -1 - \epsilon & 1 + \epsilon \end{bmatrix}, \quad (23)$$

where $0 < \epsilon < 1$. Note that when $\epsilon = 0$, $L_{asym} = L_{sym}$. Lemma 4.4: An $N \times N$ Laplacian matrix of the form (22) or (23) is diagonalizable, and its eigenvalues are given by

$$\begin{cases} \lambda_1 = 0 \\ \lambda_{i+1} = 2 + 2p \cos \frac{i\pi}{N}, i \in \{1, 2, \cdots, N-1\}, \end{cases}$$
 where $p = \sqrt{1 - \epsilon^2}$ and $0 \le \epsilon < 1$.

Proof: We use the fact that a Toeplitz matrix of the form

$$L = \begin{bmatrix} b + \gamma & c & 0 & \cdots & 0 & \alpha \\ a & b & c & & & 0 \\ 0 & \ddots & \ddots & \ddots & & \vdots \\ \vdots & & a & b & c & 0 \\ 0 & & & a & b & c \\ \beta & 0 & \cdots & 0 & a & b + \delta \end{bmatrix} . \tag{25}$$

has the eignevalues:

$$\lambda = b + 2c\rho\cos\theta,\tag{26}$$

where $\rho = \sqrt{a/c}$ and θ s are solutions to

$$\rho^{n}(ac\sin(N+1)\theta + (\gamma\delta - \alpha\beta)\sin(N-1)\theta - c\rho(\gamma+\delta)\sin N\theta) - (c\alpha\rho^{2N} + \alpha\beta)\sin \theta = 0, \quad (27)$$

with $sin(\theta) \neq 0$ [18]. Applying this to the matrices of the form (22) and (23), we obtain $a=-1-\epsilon, b=2, c=-1+\epsilon,$ $\alpha=\beta=0, \ \gamma=a, \ \delta=c, \ {\rm and} \ \rho=\sqrt{\frac{-1-\epsilon}{-1+\epsilon}}$., which leads to

$$\lambda_i = 2 - 2\sqrt{1 - \epsilon^2} \cos \theta_i, i \in \{1, 2, \dots, N\}.$$
 (28)

Equation (27) reduces to

$$2\sqrt{ac}\sin N\theta(2\sqrt{ac}\cos\theta - 1) = 0. \tag{29}$$

Solving (29) we get $\theta = \frac{i\pi}{N}$ or $\cos(\theta) = \frac{1}{2\sqrt{ac}}$, which leads to N distinct λ_i values in (28). Therefore matrices of the form (22) or (23) have N distinct eigenvalues, i.e., they are diagonalizable.

V. NUMERICAL RESULTS

In this section, we explore the influence of asymmetry on the collision potential in second order systems connected over a line graph (e.g., a linear vehicle platoon) for two scenarios; a platoon with no leader and a platoon with a leader. A system with a leader has a feedback interconnection structure the differs from the feedback laws for the two no leader cases described in (6) and (8) due to the self loop at the first node. The corresponding RPAV and RPRV feedback laws are respectively,

$$\begin{aligned} u_1 &= -\sum_{(1,j) \in \mathcal{E}} \alpha_{ij} (x_1 - x_j) - \hat{\alpha} x_1 - \beta_i v_1, \\ u_1 &= -\sum_{(1,j) \in \mathcal{E}} \alpha_{ij} (x_1 - x_j) - \hat{\alpha} x_1 - \sum_{(1,j) \in \mathcal{E}} \beta_{ij} (v_1 - v_j) - \hat{\beta} v_1. \end{aligned}$$

The interconnection structure is described by the following matrix

$$\begin{split} \hat{L}_{asym} = \\ \begin{bmatrix} 1 - \epsilon + \hat{\alpha} & -1 + \epsilon \\ -1 - \epsilon & 2 & -1 + \epsilon \\ & \ddots & \ddots & \ddots \\ & & -1 - \epsilon & 2 & -1 + \epsilon \\ & & & -1 - \epsilon & 1 + \epsilon \\ \end{bmatrix}. \end{split}$$

We perform simulations for 50 node networks using parameters $\hat{\alpha} = \hat{\beta} = 0.5$ for the leader control laws and an asymmetry offset given by $\epsilon = 0.02$. We set $L_{\alpha} = L_{\beta}$ for the RPRV control laws. We consider the following cases

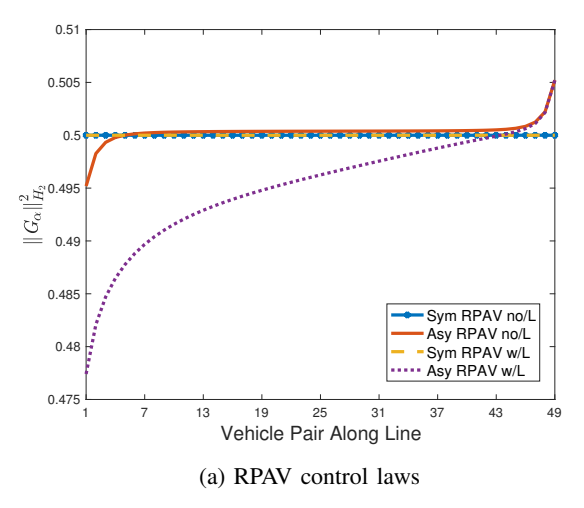
- 1) **Sym RPAV w/L**: Symmetric relative position absolute velocity control with leader
- 2) **Sym RPAV no/L**: Symmetric relative position absolute velocity control without leader
- Asy RPAV w/L: Asymmetric relative position absolute velocity control with leader
- 4) **Asy RPAV no/L**: Asymmetric relative position absolute velocity control without leader
- 5) **Sym RPRV w/L**: Symmetric relative position relative velocity control with leader
- 6) **Sym RPRV no/L**: Symmetric relative position relative velocity control without leader
- Asy RPRV w/L: Asymmetric relative position relative velocity control with leader
- 8) **Asy RPRV no/L**: Asymmetric relative position relative velocity control without leader

Figure 2 compares how the \mathcal{H}_2 norm changes along the platoon for adjacent pairs of vehicles for each of the cases. These results show that when ϵ is small, all of the cases show better performance (disturbance rejection capability) for the node pairs at the front of the platoon. However, the performance of last several nodes pairs is actually worse for systems with asymmetric control feedback.

Additional simulation results demonstrate that as we increase ϵ , the performances deteriorates rapidly, especially for the last several node pairs. For $\epsilon=0.1$, the benefits of asymmetric control laws seen at the front of the network cannot compensate for the performance deterioration experienced by the last several node pairs. Thus we can conclude that for both RPAV and RPRV control strategies, asymmetric feedback does not reduce collusion potential (robustness) in these platoons and in fact makes long platoons more vulnerable.

VI. CONCLUSIONS

We examine the collision potential for any node pair in first and second order double integrator networks with asymmetric feedback laws. We focus on the special case of systems whose feedback interconnection is described by a strongly connected digraph with a diagonalizable weighted graph Laplacian. Our main results exploit the fact that this performance measure can be computed in terms of the \mathcal{H}_2 norm of the system to find closed form expressions that describe this performance measure in terms of the eigenvalues of the graph Laplacians. Numerical examples are used to illustrate the theory for second order integrator systems communicating over a line graph (a linear vehicle platoon) with two different feedback laws. We consider networks with and without leaders, and find that the asymmetric communication graphs increase the possibility that vehicle pairs toward the rear of the platoon will collide. This decrease in system robustness is in contrast to the previously observed improved stability margin with asymmetric feedback laws.



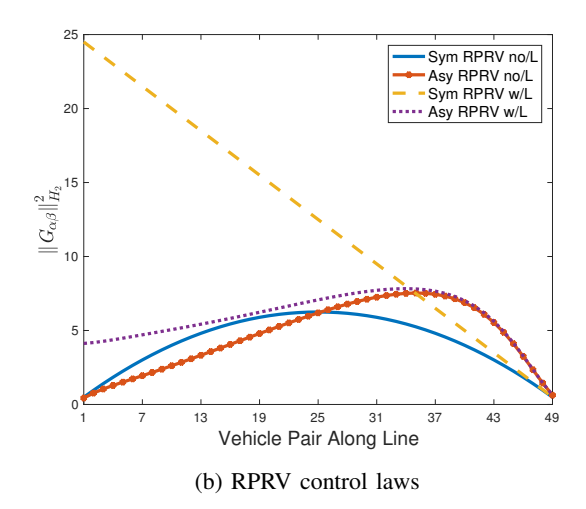


Fig. 2: The \mathcal{H}_2 norm for vehicle pairs along linear platoons for the eight different cases. In systems with and without leaders, the asymmetric control laws decrease the collision potential (increase robustness) at the front of the platoon but the benefits decrease as the platoon length increases. In fact, the performance obtained using the asymmetric feedback is worse than that for the symmetric control laws for the vehicle pairs at the end of the simulated platoon.

Characterizing vehicular and robotic networks with more general asymmetric communication graphs as well as the stability/performance trade-off is another topic of ongoing work.

ACKNOWLEDGMENTS

The authors would like to thank Theodore W. Grunberg who initiated this problem and provided insightful comments on early results. Support by the NSF (Grant number CNS 1544771) is gratefully acknowledged.

REFERENCES

- L. Xiao, S. Boyd, and S.-J. Kim, "Distributed average consensus with least-mean-square deviation," J. of Parallel and Distributed Computing, vol. 67, no. 1, pp. 33–46, Jan. 2007.
- [2] F. Dörfler and F. Bullo, "Synchronization of power networks: Network reduction and effective resistance," in *Proc. of the International Federation of Automatic Control World Congress*, vol. 43, no. 19, 2010, pp. 197 – 202.
- [3] B. Bamieh and D. F. Gayme, "The price of synchrony: Resistive losses due to phase synchronization in power networks," in *Proc. of the American Control Conf.*, Washington, DC, 2013, pp. 5815–5820.
- [4] T. Coletta and P. Jacquod, "Performance Measures in Electric Power Networks under Line Contingencies," *ArXiv e-prints*, Nov. 2017.
- [5] B. Ermentrout, "An adaptive model for synchrony in the firefly pteroptyx malaccae," *J. of Mathematical Biology*, vol. 29, no. 6, pp. 571–585, Jun 1991.
- [6] X. Liu, A. Goldsmith, S. Mahal, and J. Hedrick, "Effects of communication delay on string stability in vehicle platoons," in *Proc. of IEEE Intelligent Transportation Systems Conf.*, Aug. 2001, pp. 625–630.
- [7] D. Swaroop and J. K. Hedrick, "String stability of interconneccted systems," *IEEE Trans. on Automatic Control*, vol. 41, no. 3, pp. 349– 357, Mar. 1996.
- [8] P. Barooah, P. G. Mehta, and J. P. Hespanha, "Mistuning-based control design to improve closed-loop stability margin of vehicular platoons," *IEEE Trans. on Automatic Control*, vol. 54, no. 9, pp. 2100–2113, 2009.
- [9] H. Hao and P. Barooah, "On achieving size-independent stability margin of vehicular lattice formations with distributed control," *IEEE Trans. on Automatic Control*, vol. 57, no. 10, pp. 2688 – 2694, 2012.

- [10] B. Bamieh, M. R. Jovanović, P. Mitra, and S. Patterson, "Coherence in large-scale networks: Dimension-dependent limitations of local feedback," *IEEE Trans. on Automatic Control*, vol. 57, no. 9, pp. 2235 – 2249, 2012.
- [11] E. Tegling, B. Bamieh, and D. F. Gayme, "The price of synchrony: Evaluating the resistive losses in synchronizing power networks," *IEEE Trans. on Control of Network Systems*, vol. 2, no. 3, pp. 254 – 266, 2015.
- [12] T. W. Grunberg and D. F. Gayme, "Performance measures for linear oscillator networks over arbitrary graphs," *IEEE Trans. on Control of Network Systems*, vol. 5, no. 1, pp. 456–468, March 2018.
- [13] J. Wang, Y. Tan, and I. Mareels, "Robustness analysis of leader-follower consensus," *J. of Systems Science and Complexity*, vol. 22, no. 2, pp. 186 –206, 2009.
- [14] M. Siami and N. Motee, "Performance analysis of linear consensus networks with structured stochastic disturbance inputs," in *Proc. of the American Control Conf.*, Chicago, IL, July 2015, pp. 4080–4085.
- [15] —, "Fundamental limits on robustness measures in networks of interconnected systems," in *Proc. of the IEEE Conf. on Decision and Control*, Florence, Italy, Dec 2014, pp. 67–72.
- [16] T. W. Grunberg and D. F. Gayme, "Determining collision potential as a measure of robustness in vehicular networks," in *Proc. of the American Control Conf.*, Seattle, WA, May 2017, pp. 3992 – 3998.
- [17] H. G. Oral, E. Mallada, and D. Gayme, "Performance of first and second order linear networked systems over digraphs," in *Proc. of the* 56th IEEE Conf. on Decision and Control, Melbourne, Austrailia, Dec 2017, pp. 1688–1694.
- [18] W.-C. Yueh and S. S. Cheng, "Explicit eigenvalues and inverses of tridiagonal toeplitz matrices with four perturbed corners," *The ANZIAM Journal*, vol. 49, pp. 361–387, 2008.